4-1990

Kinetics of the Metal-Exchange Reaction between Ortho-Phospho-DL -Serinenickelate(II) and Copper(II)

Jeffrey M. Peterman

KINETICS OF THE METAL-EXCHANGE REACTION BETWEEN ORTHO-PHOSPHO-DL-SERINENICKELATE(II) AND COPPER(II)

by

Jeffrey M. Peterman

A Thesis
Submitted to the
Faculty of The Graduate College
in partial fulfillment of the
requirements for the
Degree of Master of Arts
Department of Chemistry

Western Michigan University
Kalamazoo, Michigan
April 1990

ACKNOWLEDGEMENTS

The author wishes to express his most sincere appreciation to Dr. Ralph K. Steinhaus for his valuable suggestions, patience, direction, and constructive criticism throughout the course of this study. Thanks are also given to the faculty of the Chemistry Department at Western Michigan University and especially to the members of the author's committee, Dr. James A. Howell and Dr. Dean W. Cooke.

The author wishes to express a sincere gratitude to his family, especially his parents, for their constant encouragement, understanding, and financial support during his graduate study.

Jeffrey M. Peterman

INFORMATION TO USERS

The most advanced technology has been used to photograph and reproduce this manuscript from the microfilm master. UMI films the text directly from the original or copy submitted. Thus, some thesis and dissertation copies are in typewriter face, while others may be from any type of computer printer.

The quality of this reproduction is dependent upon the quality of the copy submitted. Broken or indistinct print, colored or poor quality illustrations and photographs, print bleedthrough, substandard margins, and improper alignment can adversely affect reproduction.

In the unlikely event that the author did not send UMI a complete manuscript and there are missing pages, these will be noted. Also, if unauthorized copyright material had to be removed, a note will indicate the deletion.

Oversize materials (e.g., maps, drawings, charts) are reproduced by sectioning the original, beginning at the upper left-hand corner and continuing from left to right in equal sections with small overlaps. Each original is also photographed in one exposure and is included in reduced form at the back of the book.

Photographs included in the original manuscript have been reproduced xerographically in this copy. Higher quality 6" x 9" black and white photographic prints are available for any photographs or illustrations appearing in this copy for an additional charge. Contact UMI directly to order.

U·M·I

University Microfilms International
A Bell & Howell Information Company
300 North Zeeb Road, Ann Arbor, MI 48106-1346 USA
313/761-4700 800/521-0600

Order Number 1339921

Kinetics of the metal-exchange reaction between ortho-phospho-DL-serinenickelate(II) and copper(II)

Peterman, Jeffrey M., M.A.

Western Michigan University, 1990

U·M·I
300 N. Zeeb Rd.
Ann Arbor, MI 48106

TABLE OF CONTENTS

LIST OF TABLES

LIST OF FIGURES

INTRODUCTION

Multidentate ligand transfer between two metal ions, as represented by equation 1, has been extensively studied for a variety of metal ion and aminocarboxylate ligand combinations (1-13).

$$ML + M' \rightarrow M'L + M \qquad (1)$$

Previous papers have dealt with the characteristics of these reactions as well as forming a basis from which mechanisms and rate constants can accurately be predicted.

Most of the systems studied thus far have involved aminocarboxylate ligands, whereas only three reports of metal exchange reactions involving polyamine ligands have appeared (11,14,15). One report dealt with an interesting polyamine, N,N'-bis(2-picolyl)-ethylenediamine, having both aromatic and aliphatic dentate sites (11). The structure of this ligand and others mentioned in this thesis are illustrated in Table 1. In a recent study the metal exchange of another ligand, N-(2-pyridylmethyl) iminodiacetic acid, having both aromatic and aliphatic dentate sites was investigated as well (16).

The steric effect that a noncoordinating substituent placed on or between dentate sites of a multidentate ligand can have on a metal exchange reaction has also been studied

Table 1

Ligand Structures and Abbreviations

Ligand	Abbreviations	Ligand Structure
Ethylenediaminetetra-acetic acid	EDTA	$(HOOCCH_2)_2NCH_2CH_2N(CH_2COOH)_2$
Ethylenediamine-N,N'-diacetic acid	EDDA	$HOOCCH_2NHCH_2CH_2HNCH_2COOH$
Nitrilotriacetic acid	NTA	$N(CH_2COOH)_3$
N,N'-bis(2-picolyl) ethylenediamine	BPEDA	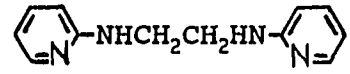
N-(2-pyridylmethyl) iminodiacetic acid	PyIDA	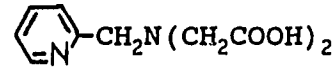
Ethylenediamine-N,N'-di-α-propionic acid	EDDP	$HOOCHC(CH_3)-NHCH_2CH_2HN-CH(CH_3)COOH$
Ortho-phospho-DL-serine	OPS	$H_2O_3P-OCH_2CH(NH_2)COOH$
N-hydroxyethylethylene-diaminetriacetic acid	HEEDTA	$HOOCCH_2NCH_2CH_2N(CH_2COOH)_2$ with CH_2CH_2OH
Triethylenetetraamine	Trien	$H_2NCH_2CH_2NHCH_2CH_2NHCH_2CH_2NH_2$

(13,17,18). Two of the studies involved substituents on the ethylene backbone of the ligand. In one case the ligand, cyclohexylenediaminetetraacetic acid, showed such a large steric effect that, for some metal pairs, no dinuclear intermediate formed (17). The second case involved a series of Schiff base ligands and again no dinuclear intermediate was postulated (18). In the other system the ligand ethylenediamine-N,N'-di-α-propionic acid, which has a methyl group on the α-carbon of each acetate arm, was investigated for possible steric effects (13). Comparison of the results with the structurally similar NiEDDA-copper system (8) showed the mechanism to be affected by the α-methyl substituents.

Another study dealt with the kinetic effect ions coordinated to the attacking metal have upon the exchange rate (9). Hydroxide appeared to significantly accelerate the exchange rate in all cases, whereas azide and acetate have relatively small effects. Subsequent studies, including this one, have shown the accelerating effect that hydrolyzed copper species have upon metal exchange reactions (10,11,13).

Detailed studies have shown the mechanism of these reactions to follow the successive breaking of a series of coordinate bonds from the original metal-ligand complex, followed by a stepwise coordination to the attacking metal

(1,2,3,5-13). This process leads to the formation of a dinuclear intermediate found in all cases where sterically possible (4,19,20), followed by breakup to form products. Depending upon the system, the position of the rate determining step has been found to be a function of pH (7,8,10), attacking metal concentration (7,8,12), the relative stability of the intermediate metal segments (3) and the relative rate of water loss from the metal complexes involved (9).

The present study is concerned with the metal exchange reaction between ortho-phospho-DL-serinenickelate(II), $NiOPS^-$, and copper(II) as shown in equation 2. This study was undertaken to determine the effect phosphate coordination has upon metal exchange.

$$NiOPS^- + Cu^{2+} \rightarrow CuOPS^- + Ni^{2+} \quad (2)$$

Ortho-phospho-DL-serine is a biologically occurring amino phosphate ester and is potentially tridentate binding through the carboxylate, phosphate, and amino moieties. The final step in the biosynthesis of serine is the hydrolysis of ortho-phosphoserine which is catalyzed by an enzyme that in turn is activated by the presence of divalent metal ions. Therefore, the reaction shown in equation 2 may have biochemical significance since metal-exchange reactions can serve as models for metallo-enzyme studies.

This study demonstrates that the reaction shown in equation 2 does proceed through the formation of a dinuclear intermediate. The rate of exchange is shown to increase with increasing pH. The increase in rate is due to $CuOH^{+}$ which is more reactive than Cu^{2+} towards nickel-phosphoserine. Evidence of a hydroxide ion attack upon water molecules coordinated to the $NiOPS^{-}$ complex is also seen. The structure of the dinuclear intermediate has been characterized by comparison of the rate constant ratios to the relative stability constant ratios using similar systems. Further, a general mechanism is proposed for the exchange reaction consistent with the kinetic data and the structure of the dinuclear intermediate.

APPARATUS AND REAGENTS

Apparatus

All spectrophotometric measurements of systems at equilibrium were made on a Cary Model 14 spectrophotometer. Typical settings were as follows: wavelength 245 nm, slit control 20, hydrogen lamp source, dynode voltage setting 2, slit height 20 mm, spectral band width 1.1 Å.

All pH measurements were made at 25.0 ± 0.1°C using either a Corning Model 12 Research pH meter or a Beckman Model 1019 pH meter. A single combination electrode was used on both pH meters. Beckman standard buffer solutions were used to standardize the pH meters.

All kinetic measurements were made on an American Instrument Company stopped-flow apparatus attached to a Shimadzu QV-50 spectrophotometer using a Beckman DU power supply. The wavelength was set at 245 nm for all kinetic measurements and the slit width varied from 1.1 to 1.7 mm. Voltage received from the photomultiplier tube was fully damped by an American Instrument Company kinetic photometer attached to a Kepco power supply set at 0.8 kv. Spectral changes were displayed on a Tektronix R5103N storage oscilloscope and recorded on Polaroid film using a Tektronix C-5 oscilloscope camera. Reservoir sites for

the reactant solutions within the stopped-flow apparatus were maintained at a constant temperature of 25.0 $\pm$ 0.1^{0}C using a circulating constant temperature bath.

Reagents

All solutions were prepared with double distilled deionized water prepared by passing distilled water through a deionizing column of Amberlite MB-3 mixed bed resin and distilled twice thereafter.

Primary Standard Copper(II) Nitrate, 0.1 M

Baker Analyzed Reagent copper foil (99.96% pure) was cleaned and rinsed with dilute nitric acid. The foil was further rinsed with distilled water followed by ethanol and air dried. A weighed portion was dissolved in a minimal amount of concentrated nitric acid and diluted to volume.

Ethylenediaminetetraacetic Acid Disodium Salt, 0.1 M

An EDTA solution was prepared from Aldrich gold label ethylenediaminetetraacetic acid, disodium salt dihydrate (99+%). The EDTA solution was standardized at pH 5 by titration against primary standard copper(II) nitrate solution using naphthylazoxine S (NAS) as the indicator.

Copper(II) Nitrate, 0.1 M

A stock copper(II) nitrate solution was prepared from Baker Analyzed Reagent copper(II) nitrate trihydrate and standardized by titration against EDTA solution at pH 5 using NAS as the indicator.

Nickel(II) Nitrate, 0.1 M

A stock nickel(II) nitrate solution was prepared from Baker Analyzed Reagent nickel(II) nitrate hexahydrate and standardized by titration against standard EDTA solution at pH 5 using NAS as the indicator.

Acetic Acid - Sodium Acetate Buffer

An acetate buffer solution, pH 5, was prepared from Fisher A.C.S. crystal sodium acetate trihydrate and Baker Analyzed Reagent glacial acetic acid (99.9% pure).

Boric Acid - Sodium Borate Buffer

A 0.1 M borate buffer solution was prepared from analytical reagent boric acid, H_3BO_3, and A.C.S. reagent grade sodium borate decahydrate, $Na_2B_4O_7 \cdot 10\text{-}H_2O$. Reagent grade D-mannitol was used to adjust the pH of the borate buffer solution.

Naphthylazoxine S Indicator, NAS

A 0.1% aqueous solution was prepared from G. Frederick Smith Naphthylazoxine S.

Sodium Perchlorate, Ionic Strength

A 5 M sodium perchlorate solution used to control ionic strength was prepared from G. Frederick Smith anhydrous reagent grade sodium perchlorate.

Ammonia Buffer, pH 10

An ammonia buffer was prepared by adding a volume of concentrated ammonium hydroxide to distilled water and adjusting the pH to 10 with dilute hydrochloric acid.

O-Phospho-DL-Serine, OPS

O-phospho-DL-serine was obtained from the Sigma Chemical Company with a reported anhydrous molecular weight of 185.1 g/mole. The purity and molecular weight of OPS as determined by potentiometric titration with standard carbonate-free sodium hydroxide solution was 99.6% and 185.82 respectively. These values were calculated from the 2nd equivalence point of the potentiometric titration curve shown in Figure 1.

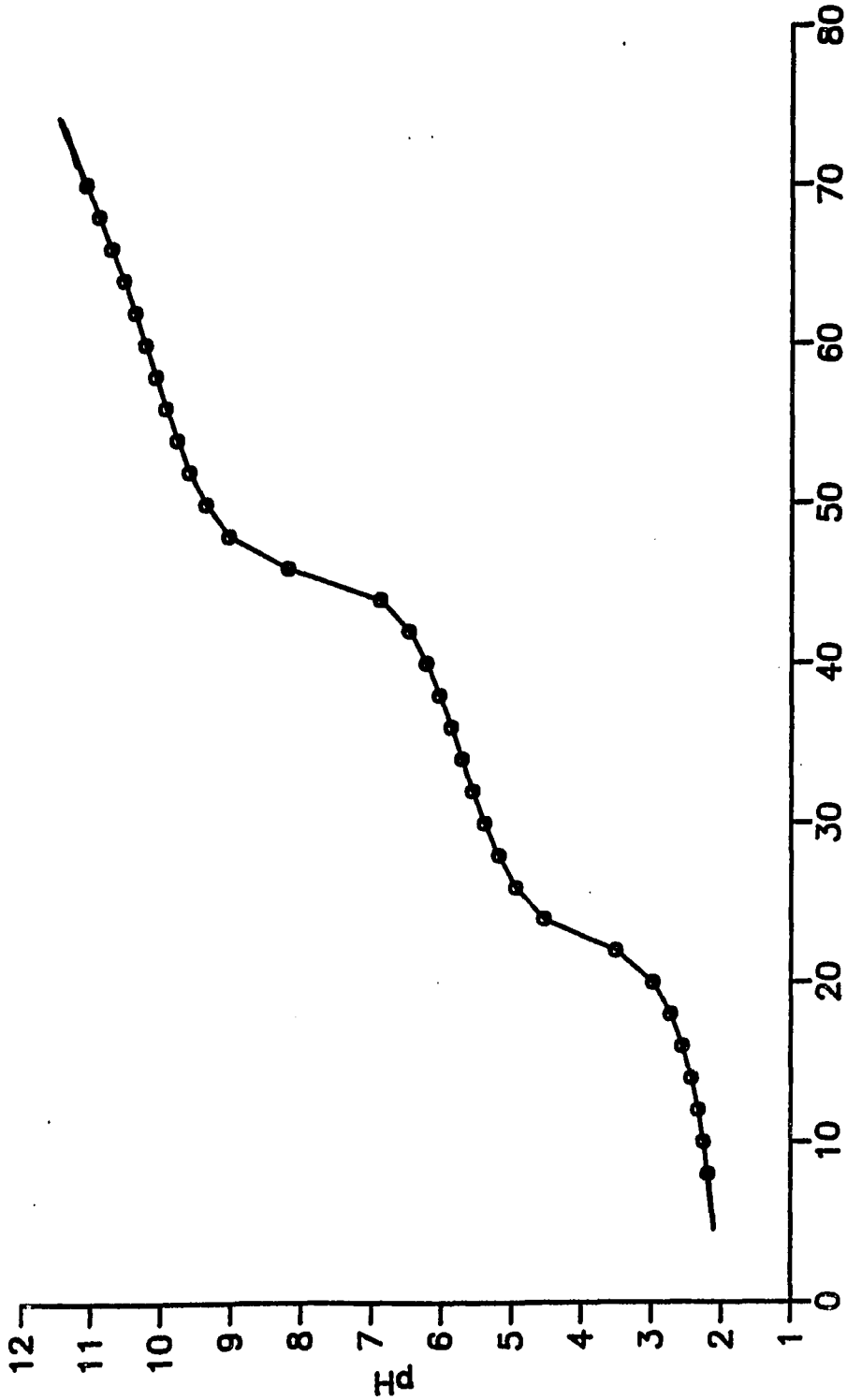

Figure 1. Potentiometric Titration of O-Phospho-DL-Serine With 0.1M Sodium Hydroxide.

O-Phospho-DL-Serinenickelate(II), $NiOPS^-$

A 0.05 M $NiOPS^-$ solution was prepared by mixing equimolar volumes of nickel(II) nitrate and O-phospho-DL-serine stock solutions. The $NiOPS^-$ solution was standardized spectrophotometrically by adding 100-fold excess sodium cyanide at pH 10 to form the tetracyanonickel(II) complex and the comparing the absorbance at 267 nm with that of a standard $Ni(CN)_4^{2-}$ solution.

EXPERIMENTAL

Spectrophotometric Study of Reactants and Products

The absorption spectra of all reactants and products were obtained from 200 nm to 400 nm. These spectra showed the largest differences in molar absorptivity between reactants and products to be within the wavelength range of 240 nm to 250 nm. Through trial kinetic runs a wavelength of 245 nm was chosen to follow the course of the reaction. All kinetic measurements were made at this wavelength. This corresponds to the maximum absorption of products, $CuOPS^-$ and CuHOPS, with minimal contribution from the other species.

The molar absorptivities of all species were determined at 245 nm and are listed in Table 2. The ionic strength of all solutions was adjusted to 0.1 M with sodium perchlorate solution.

Reaction Conditions and Rates

The reaction in equation 2 was studied by measuring the increase in the absorbance due to the formation of $CuOPS^-$ and CuHOPS. A boric acid - sodium borate buffer was used to maintain a constant pH. The pH of the reaction was

Table 2

Molar Absorptivities of Reactants and Products

Species	ϵ, L mol^{-1} cm^{-1}
Ni^{2+}	62.4
Cu^{2+}	98.3
$NiOPS^-$	852
NiHOPS	237
$CuOPS^-$	1585
CuHOPS	2437

Note. λ = 245 nm, μ = 0.1 M

measured by mixing 5 ml of each reactant solution adjusted to the same pH. In all cases there was little or no change in pH upon mixing. The pH range over which kinetic measurements could be made was limited at higher pH by the formation of a copper(II) hydroxide precipitate and at lower pH by the lack of a suitable buffer.

The kinetic measurements were made under pseudo-first-order conditions in which the total copper(II) concentration was present in at least a 10-fold excess over that of nickel-phosphoserine. Each reported kinetic run is for a specific set of reaction conditions and is the average

of at least 4 separate stopped-flow runs. The experimental conditions used in all reaction rate studies are given in Table 3.

Table 3

Experimental Conditions

$[NiOPS]_{total}$	2.56×10^{-5} M, 2.65×10^{-5} M
$[Cu^{2+}]$	2.61×10^{-4} M to 1.32×10^{-3} M
pH range	3.96 to 5.20
Wavelength	245 nm
Temperature	$25.0 \pm 0.1^{0}C$
Ionic strength, μ	0.1 M

The nickel-phosphoserine reactant solutions were prepared by adding a volume of stock $NiOPS_{total}$ into a 150 ml beaker and enough sodium perchlorate solution was added to give an ionic strength of 0.1 M upon dilution to the final volume. An approximately 10-fold excess concentration of nickel(II) over the concentration of $NiOPS_{total}$ was added to increase the concentration of phosphoserine coordinated to nickel(II). Following the addition of 10 ml borate buffer the volume was increased to around 90 ml and the pH adjusted through the addition of mannitol to the desired value. This solution was transferred to a 100 ml volumetric flask

and diluted to volume. The resulting nickel-phosphoserine reactant solution was transferred back into a 150 ml beaker, placed in a constant temperature bath at 25.0 ± 0.1°C and allowed to equilibrate.

The copper(II) reactant solutions were prepared by adding a volume of stock copper(II) nitrate into a 150 ml beaker and enough sodium perchlorate solution to give an ionic strength of 0.1 M upon dilution to the final volume. Following the addition of 10 ml borate buffer the volume was increased to around 90 ml and the pH adjusted through the addition of mannitol to the desired value. This solution was transferred to a 100 ml volumetric flask and diluted to volume. The resulting copper(II) reactant solution was then transferred back into a 150 ml beaker, placed in a constant temperature bath at 25.0 ± 0.1°C and allowed to equilibrate. Both copper(II) and nickel-phosphoserine solutions were allowed to equilibrate for at least 20 minutes in the thermostated waterbath before being used.

The spectrophotometer and oscilloscope were allowed to warm-up for at least 20 minutes prior to use. With distilled water in the stopped-flow cell the oscilloscope was calibrated to full scale deflection for 0% T and 100% T. Syringes were then used to fill the reservoir sites within the stopped-flow apparatus with the nickel-phospho-

serine and copper(II) reactant solutions. A preliminary run was performed in order to obtain a value for the final percent transmittance read from the oscilloscope trace. For each set of reaction conditions the formation of copper-phosphoserine was followed by measurement of percent transmittance (%T) versus time (t). The resulting oscilloscope traces were recorded on Polaroid film. These traces were used to obtain the values of %T and time. These data were used in an iterative curve-fitting program to obtain values of the observed pseudo-first-order rate constants.

RESULTS

Kinetic Expression for the Reaction

The rate expression for the reaction $NiOPS^-$ and copper may be expressed by the following second-order equation

$$\frac{-d[NiOPS^-]}{dt} = \frac{d[CuOPS^-]}{dt} = k[NiOPS^-][Cu_T] \qquad (3)$$

where Cu_T refers to the sum of the individual copper species present. Assuming a constant copper concentration due to a 10-fold or greater excess equation 3 reduces to the pseudo-first-order equation

$$\frac{-d[NiOPS^-]}{dt} = \frac{d[CuOPS^-]}{dt} = k_0[NiOPS^-] \qquad (4)$$

where k_0 represents the observed pseudo-first-order rate constant.

$$k_0 = k[Cu_T] \qquad (5)$$

The integrated form of equation 4 yields

$$\ln[NiOPS^-]_t = \ln[NiOPS^-]_0 - k_0 t \qquad (6)$$

where $[NiOPS^-]_t$ is the concentration of $NiOPS^-$ at time t, and $[NiOPS^-]_0$ is the initial concentration. The loss of $NiOPS^-$ is inversely proportional to the formation of $CuOPS^-$ and related to the change in absorbance as the reaction progresses. Equation 7 relates the final absorbance, A_∞, the absorbance at any time, A_t, the molar absorptivities of reactants and products, ϵ, and the cell path length, b, to

the concentration of $NiOPS^-$. The derivation of equation 7 is given in Appendix A.

$$[NiOPS^-]_t = \frac{A_t - A_\infty}{b(\epsilon_{NiOPS^-} + \epsilon_{Cu^{2+}} - \epsilon_{CuOPS^-} - \epsilon_{Ni^{2+}})} \quad (7)$$

In order to show the absence of any stable intermediates in the exchange reaction, expected absorbance values were compared to observed absorbance values as shown in Table 9 in Appendix B. No evidence of any stable intermediates is found since the difference between observed and expected absorbances, ΔA, is nearly identical over 6 half-lives. The consistent difference between expected and observed absorbance values can be attributed to the fact that molar absorptivites used to calculate the expected absorbance values were determined on an instrument other than the one from which absorbances were observed.

The oscilloscope traces were used to obtain values of %T and time. From trace data, plots of $-\ln (A_\infty - A_t)$ versus time were constructed. The plots were linear demonstrating that the reaction in equation 2 is first-order in $NiOPS^-$. A typical plot is shown in Figure 2.

After the kinetic behavior was well established, an iterative curve-fitting program was used to convert the %T - time data for each run into pseudo-first-order rate constants. The program gave the best least-squares fit to

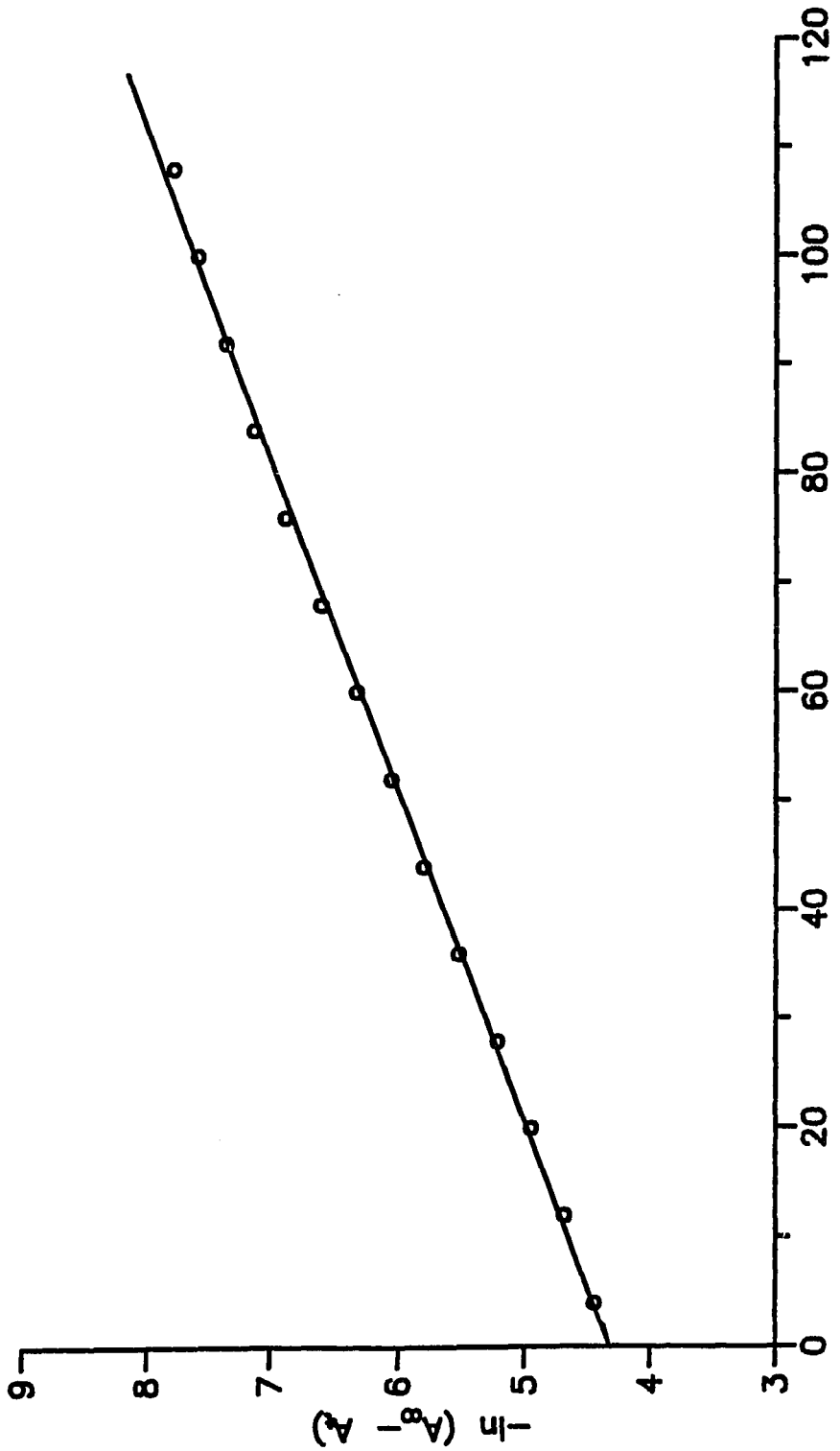

Figure 2. Typical First Order Plot of k_o at Constant Copper Concentration.

equation 8, where A_∞ is the final absorbance of the reaction and A_1 is the change in absorbance that the reaction experienced.

$$A_t = A_1 e^{-kt} + A_\infty \qquad (8)$$

The order in copper was obtained by monitoring reactions at a constant hydrogen ion concentration in which the copper concentration was varied between a 10- and a 50-fold molar excess over $[NiOPS]_{total}$. Table 4 lists the data. Figure 3 demonstrates the linearity of the plots obtained from the data in Table 4.

The effect of pH variation upon the rate is also seen in Figure 3, which demonstrates that the exchange reaction is pH sensitive since the observed rate constants increase with increasing pH values. The pH range studied was between pH 4.04 and 4.81.

Resolution of Rate Constants

The reaction between $NiOPS_{total}$ and copper(II) can be represented in general by equation 9 where the acid forms of the complexes are in rapid equilibrium with each other. Mohan and Abbott have concluded from 1:2 Ni(II)-ligand titration curves and phosphorus magnetic resonance

$$\begin{bmatrix} NiL^- \\ \uparrow\downarrow \\ NiHL \end{bmatrix} + Cu^{2+} \rightleftharpoons \begin{bmatrix} CuL^- \\ \uparrow\downarrow \\ CuHL \end{bmatrix} + Ni^{2+} \qquad (9)$$

Table 4

Values of k_0 as a Function of pH and Copper(II) Concentration[a]

pH	$[Cu_T]$, M	k_0, sec^{-1}
4.050	2.64×10^{-4}	27.04 ± 1.73
4.020	3.96×10^{-4}	27.48 ± 3.32
4.040	5.28×10^{-4}	30.28 ± 2.96
4.035	6.60×10^{-4}	28.95 ± 1.45
4.065	7.92×10^{-4}	32.27 ± 3.43
4.032	9.24×10^{-4}	34.08 ± 2.14
4.050	1.06×10^{-3}	33.49 ± 4.30
4.030	1.19×10^{-3}	38.76 ± 1.38
4.040	1.32×10^{-3}	41.70 ± 4.30
4.218	2.63×10^{-4}	34.06 ± 5.15
4.208	3.96×10^{-4}	36.30 ± 2.81
4.217[b]	5.23×10^{-4}	40.83 ± 3.00
4.212	6.60×10^{-4}	38.46 ± 1.37
4.233[b]	7.84×10^{-4}	45.34 ± 4.28
4.213	9.24×10^{-4}	48.06 ± 3.49
4.223	1.06×10^{-3}	48.38 ± 4.18
4.215	1.19×10^{-3}	49.81 ± 3.41
4.228	1.32×10^{-3}	58.06 ± 5.94
4.602[b]	2.61×10^{-4}	44.53 ± 2.05
4.610	3.96×10^{-4}	50.38 ± 5.28
4.617[b]	5.23×10^{-4}	53.25 ± 4.75
4.613	6.60×10^{-4}	64.04 ± 4.69
4.611[b]	7.84×10^{-4}	61.83 ± 4.09
4.615	9.24×10^{-4}	65.03 ± 6.64

Table 4--Continued

pH	$[Cu_T]$, M	k_0, sec^{-1}
4.616[b]	1.05×10^{-3}	67.34 ± 2.96
4.618	1.19×10^{-3}	84.34 ± 7.81
4.607[b]	1.31×10^{-3}	77.61 ± 7.33
4.818[b]	2.61×10^{-4}	52.39 ± 2.09
4.805	3.96×10^{-4}	62.78 ± 5.19
4.811	5.25×10^{-4}	62.01 ± 5.83
4.802	6.06×10^{-4}	66.97 ± 4.49
4.808[b]	7.83×10^{-4}	68.75 ± 4.96
4.805	9.24×10^{-4}	75.71 ± 7.11
4.795	1.06×10^{-3}	81.72 ± 7.65
4.811	1.19×10^{-3}	101.11 ± 20.82
4.808	1.32×10^{-3}	99.95 ± 8.51

[a] All values at $[NiOPS]_{total} = 2.65 \times 10^{-5}$ M, μ = 0.1 M, T = 25.0 ± 0.1° C except as noted.

[b] $[NiOPS]_{total} = 2.56 \times 10^{-5}$ M, μ = 0.1 M, T = 25.0 ± 0.1° C.

(^{31}P NMR) evidence that in the unprotonated $NiOPS^-$ complex the ligand is tricoordinate to nickel (21).

The effect of a change in copper concentration at four pH values is shown in Figure 3. A linear dependence of the observed rate constant on copper concentration was found throughout the entire copper concentration range studied.

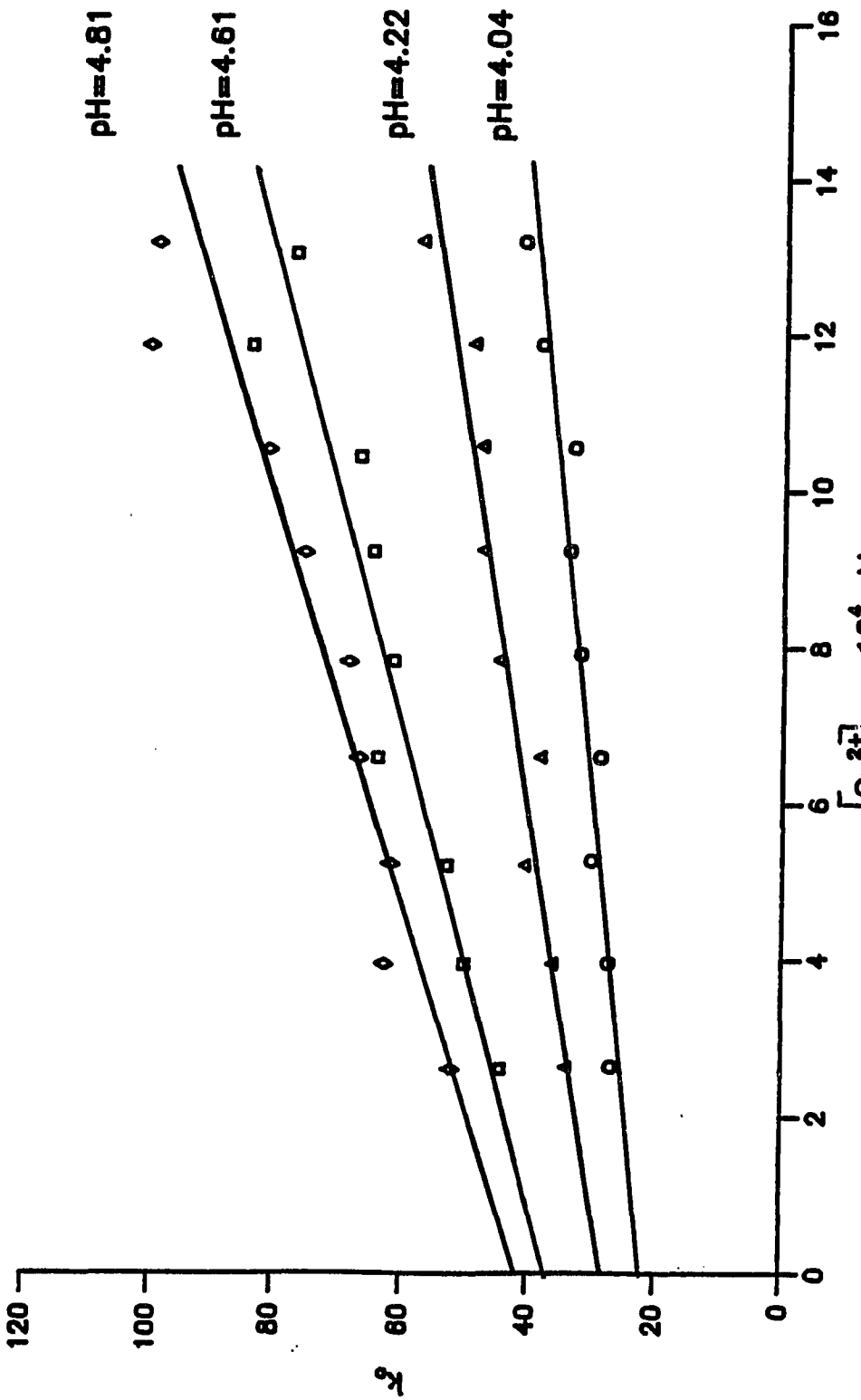

Figure 3. Effect of Copper Concentration and pH on k_o.

Figure 3 indicates that the exchange reaction is pH sensitive since the rate increases with increasing pH. However, the rate varies inversely with $[H^+]$, not directly as would be expected if hydrogen ion were the attacking species or if NiHOPS were a reactive species. This pH behavior rules out a hydrogen dependent term involving NiHOPS. Figure 3 also illustrates that the rate increases with increasing copper concentration and that there is a copper dependent term that is pH dependent because the slopes at each pH are different. In addition, Figure 3 shows a copper independent term that is pH dependent because the intercepts at each pH are different.

Figure 4 shows a least-squares plot of the four slopes from Figure 3 versus $1/[H^+]$. The positive slope indicates that there is a copper dependent term that varies inversely with hydrogen ion concentration and the intercept indicates a copper dependent pH independent term for the exchange reaction.

An explanation for the inverse $[H^+]$ behavior of the copper dependent term involves the attack of a hydrolyzed copper species on the nickel-phosphoserine complex. There is both kinetic and thermodynamic evidence for the existence of hydrolyzed copper species. Many hydrolyzed copper complexes exist, for example $CuOH^+$, $Cu_2(OH)_2^{2+}$, Cu_2OH^{3+}, $Cu_3(OH)_2^{4+}$, and $Cu_n(OH)_{2n-2}^{2+}$ (22,23,24). Formation

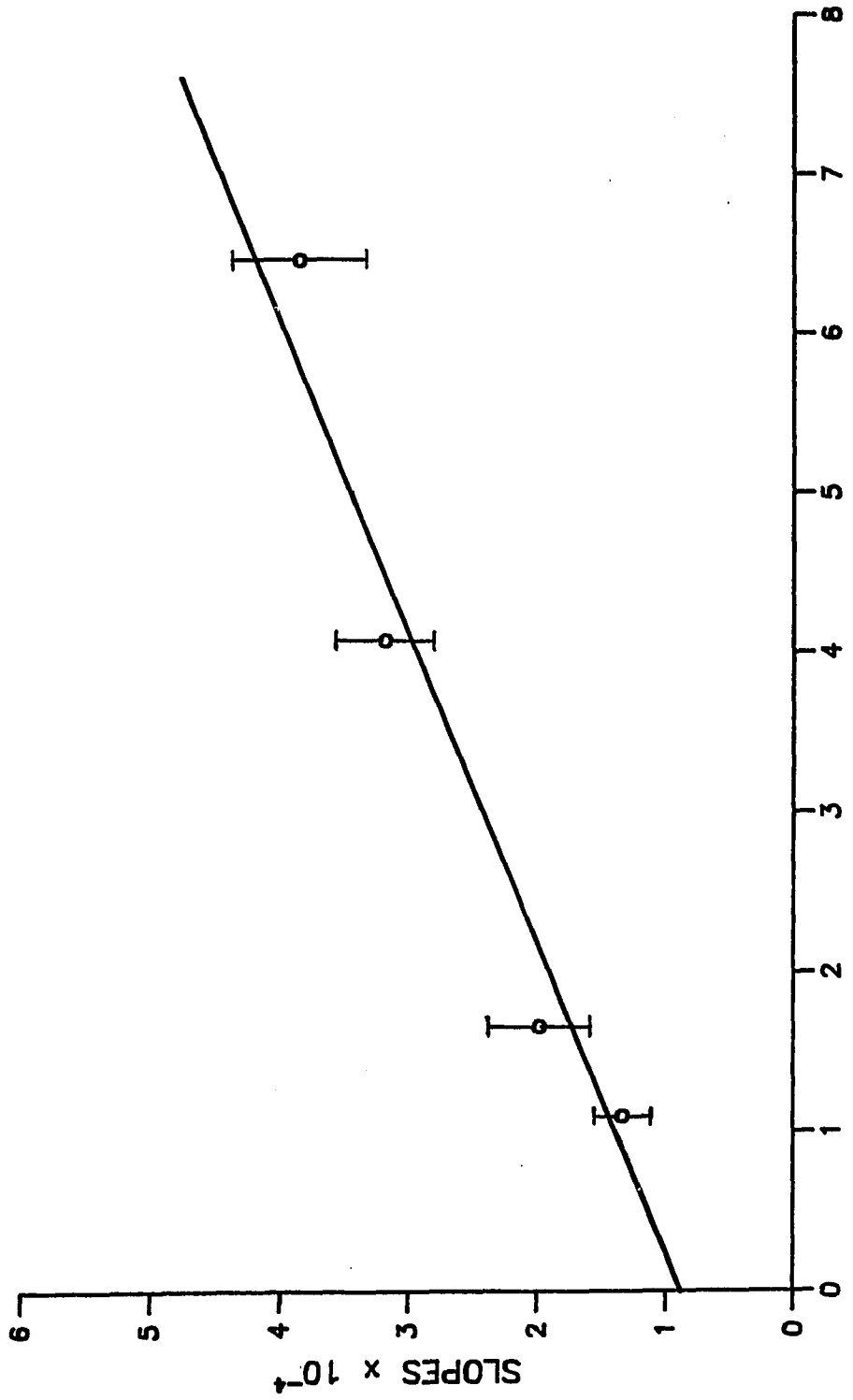

Figure 4. Resolution of Copper Dependent Terms.

constants are known for all the above copper hydroxide species.

The four differing intercepts from Figure 3 indicate that there is copper independent term that is pH dependent for the exchange process. Since the intercepts increase as hydrogen ion concentration decreases, a logical explanation for this behavior would be the attack of hydroxide ion on the nickel-phosphoserine complex.

Figure 5 shows a least-squares plot of the four intercepts from Figure 3 versus $K_W/[H^+]$. The positive slope indicates that there is a copper independent term that varies with hydroxide ion concentration and the intercept indicates a copper independent pH independent dissociation of the nickel-phosphoserine complex.

Assuming the existence and kinetic activity of $CuOH^+$ and the attack of hydroxide ion on the nickel-phosphoserine complex to be the explanation for the pH behavior seen, equation 10, a complete rate equation for metal exchange, showing all possible terms can be written.

$$k_0[NiOPS^-] = k^{NiOPS}_{Cu^{2+}}[NiOPS^-][Cu^{2+}] + k^{NiOPS}_{CuOH^+}[NiOPS^-][CuOH^+] + k^{NiOPS}_{OH^-}[NiOPS^-][OH^-] + k^{NiOPS}[NiOPS^-] \quad (10)$$

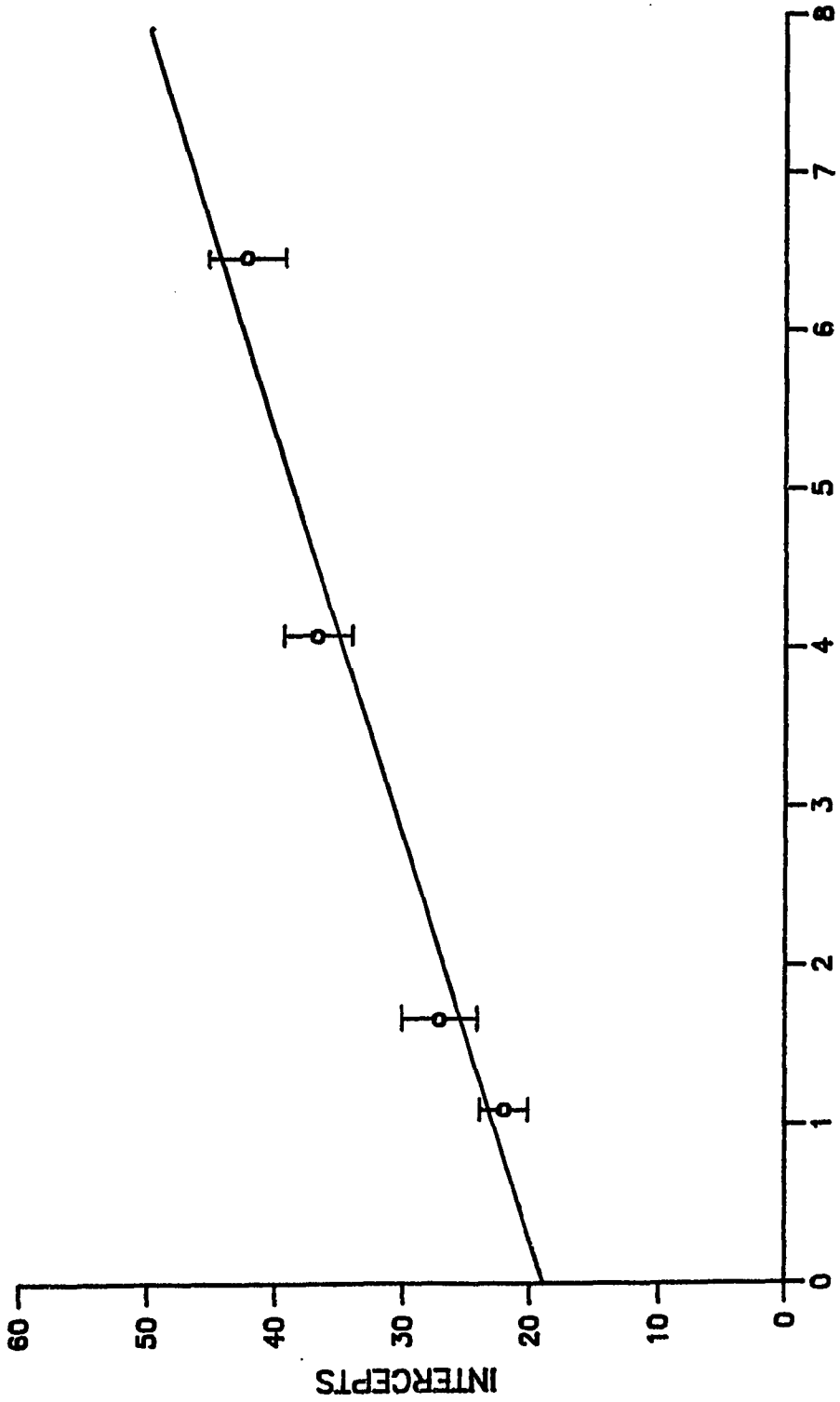

Figure 5. Resolution of Copper Independent Terms.

By use of the relations

$$Cu^{2+} + H_2O \rightarrow CuOH^+ + H^+ \quad (11)$$

for which

$$B_{11} = \frac{[CuOH^+][H^+]}{[Cu^{2+}]} \quad (12)$$

and

$$K_W = [OH^-][H^+] \quad (13)$$

equation 10 may be simplified and rewritten

$$k_0 = (k^{NiOPS}_{Cu^{2+}} + k^{NiOPS}_{CuOH^+} \frac{B_{11}}{[H^+]})[Cu^{2+}] + k^{NiOPS}_{OH^-} \frac{K_W}{[H^+]} + k^{NiOPS} \quad (14)$$

Using equation 15, the free copper concentration at any pH can be calculated from the total copper concentration and from known values of the formation constants for each species corrected to 0.1 M ionic strength. The corrected values as determined by Ohtaki and Kawai (22) are $B_{11} = 5.0 \times 10^{-8}$, $B_{21} = 1.4 \times 10^{-6}$, and $B_{22} = 2.5 \times 10^{-11}$ which correspond to equations 11, 16, and 17 respectively. Figure 3 shows a weighted least-squares plot of k_0 versus free copper concentration at four different pH values.

$$Cu_T = [Cu^{2+}] + [CuOH^+] + 2[Cu_2OH^{3+}] + 2[Cu_2(OH)_2^{2+}] \quad (15)$$

$$2Cu^{2+} + H_2O \rightarrow Cu_2OH^{3+} + H^+ \quad (16)$$

$$2Cu^{2+} + 2H_2O \rightarrow Cu_2(OH)_2^{2+} + 2H^+ \quad (17)$$

The values of the copper dependent terms, k^{NiOPS} and $k^{NiOPS}_{CuOH^+}$, were resolved from Figure 4 using equation 18. The values obtained from weighted linear least-squares analysis of Figure 4 were $k^{NiOPS}_{Cu^{2+}} = (8.80 \pm 2.54) \times 10^3\ M^{-1}\ s^{-1}$ and $k^{NiOPS}_{CuOH^+} = (1.02 \pm 0.18) \times 10^7\ M^{-1}\ s^{-1}$.

$$\text{Slope} = k^{NiOPS}_{Cu^{2+}} + k^{NiOPS}_{CuOH^+} \frac{B_{11}}{[H^+]} \qquad (18)$$

The values of the copper independent terms, $k^{NiOPS}_{OH^-}$ and k^{NiOPS}, were resolved from Figure 5 using equation 19. The values obtained from linear least-squares analysis of Figure 5 were $k^{NiOPS}_{OH^-} = (3.91 \pm 0.59) \times 10^{10}\ m^{-1}\ s^{-1}$ and $k^{NiOPS} = 18.8 \pm 2.0\ s^{-1}$. The resolved rate constants are listed in Table 5.

Table 5

Resolved Rate Constants for the Reaction of $NiOPS^-$ and Copper(II)

$k^{NiOPS}_{Cu^{2+}}$	$(8.80 \pm 2.54) \times 10^3\ M^{-1}s^{-1}$
$k^{NiOPS}_{Cu^{2+}}$	$(1.02 \pm 0.18) \times 10^7\ M^{-1}s^{-1}$
$k^{NiOPS}_{OH^-}$	$(3.91 \pm 0.59) \times 10^{10}\ M^{-1}s^{-1}$
k^{NiOPS}	$18.8 \pm 2.0\ s^{-1}$

Note. Temp. = 25.0 ± 0.1^0C, $\mu = 0.1M$

$$\text{Intercept} = k^{NiOPS}_{OH^-} \frac{K_w}{[H^+]} + k^{NiOPS} \qquad (19)$$

The resolved values of the rate constants can be used to construct a theoretical curve of k_0 and pH using equation 14 at a 10-fold excess copper(II) concentration. The theoretical curve is compared to experimentally determined values between pH 3.96 and 5.20 in Figure 6. Table 6 lists the data. Good agreement is seen over the entire pH range studied.

Table 6

Values of k_0 as a Function of pH at 10-fold Excess Copper(II) Concentration[a]

pH	k_0, sec^{-1}
3.965	29.31 ± 2.44
4.050[b]	27.04 ± 1.73
4.090	30.80 ± 1.29
4.218	34.06 ± 5.15
4.321[b]	33.81 ± 3.70
4.408	34.51 ± 1.99
4.522	41.80 ± 5.20
4.602	44.53 ± 2.05
4.818	52.39 ± 2.09
4.880	56.93 ± 5.32
5.010[b]	69.46 ± 5.56
5.205[b]	89.32 ± 4.18

[a] All values at $[Cu_T] = 2.61 \times 10^{-4}$ M, μ = 0.1 M, T = 25.0 ± 0.1° C except as noted.

[b] $[Cu_T] = 2.64 \times 10^{-4}$ M, μ = 0.1 M, T = 25.0 ± 0.1° C.

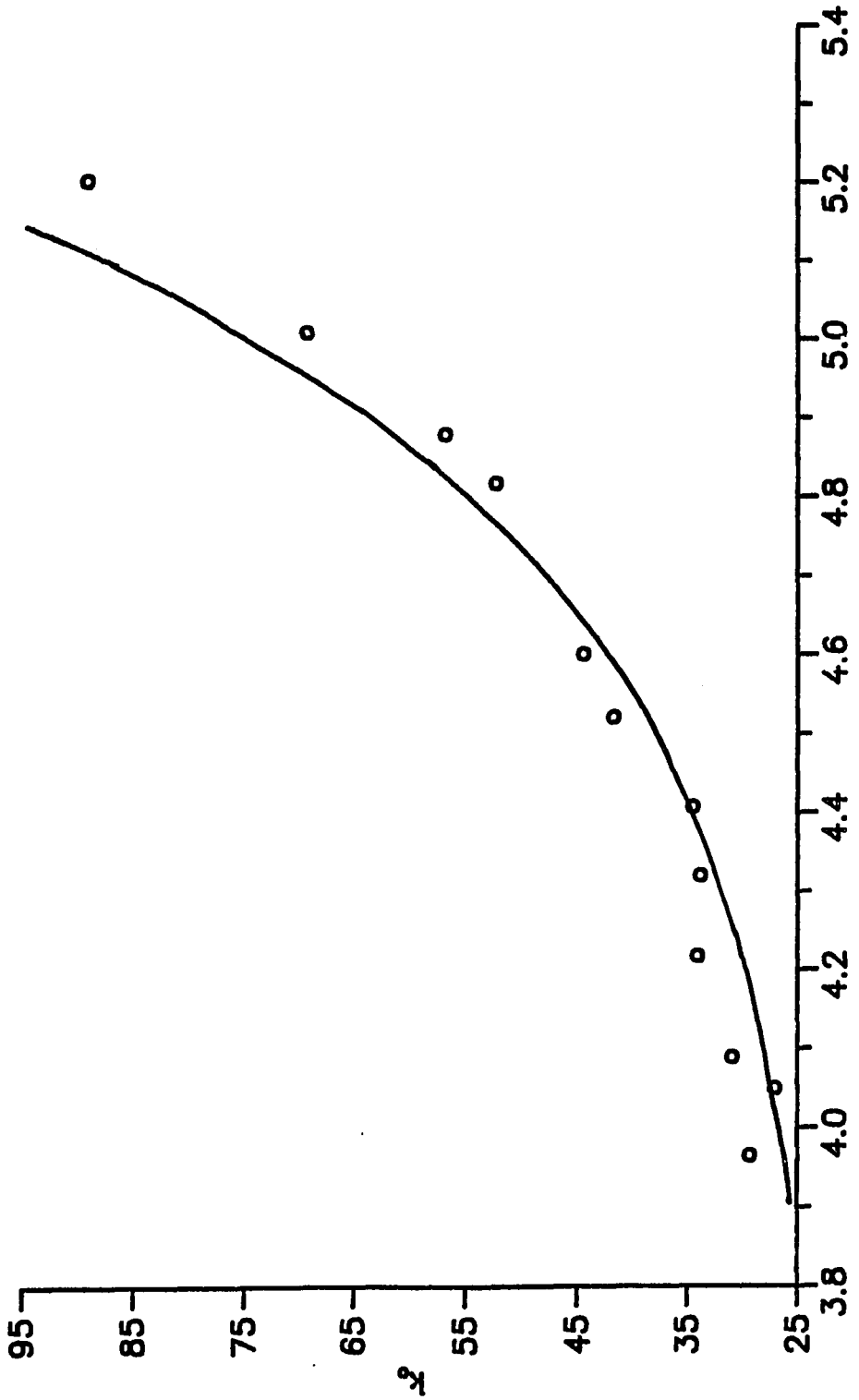

Figure 6. Comparison of Theoretical Curve to Experimentally Determined Values of k_o at 10-fold Excess Copper(II) Concentration.

DISCUSSION

The exchange reaction between $NiOPS^-$ and copper(II) appears to proceed through three different pathways: (a) a complete dissociation of $NiOPS^-$ followed by attack of copper, a pathway represented by k^{NiOPS}, (b) a copper independent hydroxide ion attack on $NiOPS^-$ followed by copper attack, the pathway represented by $k^{NiOPS}_{OH^-}$, and (c) an attack by either copper(II) ion or $CuOH^+$ on $NiOPS^-$ to yield a dinuclear intermediate, pathways represented by $k^{NiOPS}_{Cu^{2+}}$ or $k^{NiOPS}_{CuOH^+}$.

The structure of the dinuclear intermediate immediately prior to the rate determining step may be confirmed by comparing the ratio of relative stability constants involving similar systems to the ratio of experimental rate constants for metal attack for the same systems as shown in equation 20.

$$\frac{k^{NiOPS}_{Cu}}{k^{NiL}_{Cu}} = \frac{K^{Ni(OPS)Cu}_{R}}{K^{Ni(L)Cu}_{R}} \qquad (20)$$

Previous work (3,5,8,11,12,13,16) has shown that the ratio of experimental rate constants is directly proportional to the ratio of dinuclear intermediate stability constants assuming the same rate-determining step to hold for both systems. If the dinuclear intermediates have different rate-determining steps, a ratio of rate constants for the different bond cleavages is used to correct for the difference.

The relative stability constant, K_R, for each dinuclear intermediate is defined in terms of the stability of the Ni-ligand and Cu-ligand segments involved as compared to the stability of the initial Ni-ligand complex.

$$K_R = \frac{K_{\text{Ni-segment}} \times K_{\text{Cu-segment}}}{K_{\text{Ni-complex}}} \qquad (21)$$

The values of K_R were calculated from known stability constants chosen to be as internally consistent as possible with respect to temperature and ionic strength and are listed in Table 7 along with experimental values of the rate constants. Table 8 lists the comparisons between the known structures and three possible dinuclear intermediate structures for the exchange of the nickel-phosphoserine with copper(II).

In some comparisons an electrostatic attraction or repulsion helps stabilize one intermediate relative to the

Table 7

Stability and Rate Constants Used in Making Comparisons of Likely Dinuclear Intermediates[a]

Complex	K_{stab}	M	k_{Cu}^{NiL}, $M^{-1}s^{-1}$
NiEDDA	4.46×10^{13}	Cu	7.5×10^{-2} [b]
$NiEDTA^{2-}$	3.31×10^{18}	Cu	1.6×10^{-2} [c]
$NiNTA^{-}$	3.16×10^{11}	Cu	1.39×10^{-3} [d]
NiHEEDTA	1.25×10^{17}	Cu	1.5×10^{-2} [e]
$NiOPS^{-}$	2.09×10^{6} [g]	Cu	9.5×10^{-3} [f]
Intermediate metal segment			
$Ni(acetate)^{+}$	5.5		
$Ni(glycine)^{+}$	6.03×10^{5}		
$Ni(alanine)^{+}$	2.51×10^{5}		
Ni(methylphosphate)	8.13×10^{1}		
Ni(o-phosphoethanolamine)	7.41×10^{1}		
$Ni(NH_3)^{2+}$	5.01×10^{2}		
$Cu(acetate)^{+}$	6.76×10^{1}		
$Cu(glycine)^{+}$	1.41×10^{8}		
$Cu(alanine)^{+}$	1.35×10^{8}		
$Cu(OPS)^{-}$	2.51×10^{9} [g]		
Cu(o-phosphate)	1.58×10^{3}		
$Cu(NH_3)^{2+}$	1.74×10^{4}		

[a] All values are at 25.0°C and μ = 0.1M or chosen to be as close to these conditions as possible. Except as noted all values are taken from References 25, 26, 30.

[b] Reference 8.

[c] Reference 7.

[d] Reference 5.

[e] Reference 3.

[f] This work.

[g] Reference 31.

Table 8

Comparison of Possible Dinuclear Intermediates for the Exchange of $NiOPS^-$ With Cu(II) to Known Systems

Structures to be Tested	K_R	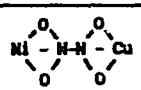 Ni(EDTA)Cu K_R = 1.50	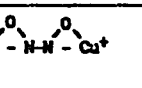 Ni(EDDA)Cu K_R = 1.91	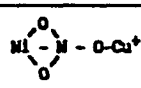 Ni(NTA)Cu K_R = 0.0286	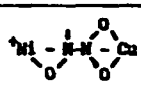 Ni(HEEDTA)Cu K_R = 0.448
		$\frac{K_R\ Ni(OPS)Cu}{K_R\ Ni(EDTA)Cu}$	$\frac{K_R\ Ni(OPS)Cu}{K_R\ Ni(EDDA)Cu}$	$\frac{K_R\ Ni(OPS)Cu}{K_R\ Ni(NTA)Cu}$	$\frac{K_R\ Ni(OPS)Cu}{K_R\ Ni(HEEDTA)Cu}$
I. 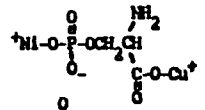	2.63×10^{-3}	1.74×10^{-1} [a,d]	2.73×10^{-1} [b,d]	1.22×10^{1} [c,d]	11.7×10^{-1} [b,d]
II. 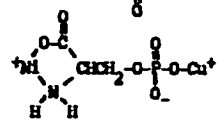	1.91×10^{2}	3.18×10^{1} [a]	5.0×10^{1} [b]	2.23×10^{3} [c]	2.13×10^{2} [b]
III. 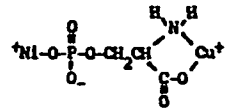	5.25×10^{3}	6.95×10^{5} [b,d]	1.09×10^{6} [d]	4.86×10^{7} [d,e]	4.65×10^{6} [d]
		5.72×10^{5}	1.22×10^{5}	6.58×10^{6}	6.10×10^{5}

Note. K_R values are based on the stability constants given in Table 7 and chosen to be as internally consistent as possible with respect to temperature and ionic strength. The experimental ratios of rate constants are based upon the rate constants given in Table 7, with u = 0.1M and T = 25.0°C. [a] Statistical factor 1/4. [b] Statistical factor 1/2. [c] Statistical factor 1/3. [d] $k_{Ni\text{-}phosphate} / k_{Ni\text{-}NH_3} = 397$. [e] Statistical factor 2/3.

other. The added stability of this contribution is an electrostatic factor, K_{el}, which can be estimated using equation 22 where Z_A and Z_B are the charges involved, e is the electronic charge, D is the dielectric constant of water, r_{AB} is the charge separation estimated from molecular models, T is the temperature in Kelvin, and R is the gas constant.

$$\log K_{el} = \frac{Z_A \, Z_B \, e^2}{2.303 \; R \; T \; D \; r_{AB}} \qquad (22)$$

There may also be a statistical factor which favors the formation of one intermediate relative to another and this term must be included in making comparisons.

Structures I and II involve cleavage of a nickel-oxygen bond as the rate determining step whereas all the structures to which it is being compared have nickel-nitrogen bond breakage as rate determining. A factor of 397 is used to compensate for this difference and is obtained from the ratio of nickel-methylphosphate dissociation, 3570 s^{-1}, and nickel-amine dissociation, 9 s^{-1}. These dissociation constants, k_d, were determined from known stability constants (25,26) and experimental formation rate constants, k_f, for nickel-methylphosphate, 2.9 x 10^5 s^{-1}, (27) and nickel-amine, 4.5 x 10^3 s^{-1} (28,29) using equation 23.

$$K_{stab} = \frac{k_f}{k_d} \qquad (23)$$

Values of K_{el}, statistical factors, and a factor to compensate the difference between cleavage of a nickel-oxygen bond compared to that of a nickel-nitrogen bond are included where appropriate. The last row in Table 8 shows the ratios of experimental rate constants. A comparison of the ratio of experimental rate constants to the predicted ratios of intermediate stability constants shows that only structure III gives predicted values that agree closely to the experimental rate constant ratios. Other structures listed in Table 8 as well as some not listed were tested and gave values which differed by several orders of magnitude.

Structure III, the proposed structure of the dinuclear intermediate, consists of nickel bonded to a phosphate oxygen and copper bonding to the glycine segment of OPS. This is much like the dinuclear intermediate found in other polyaminocarboxylate exchange reactions, with the exception being the NiNTA-Cu intermediate as shown in Table 8.

Knowledge of the structure of the dinuclear intermediate allows a mechanism to be postulated for the metal-exchange of $NiOPS^-$ and copper. This is shown in Figure 7. The reaction pathway 1 → 2 → 4 represents k^{NiOPS} with k_{12} being the rate determining step. The pathway 1 → 3 → 4, proceeding through the dinuclear intermediate, represents

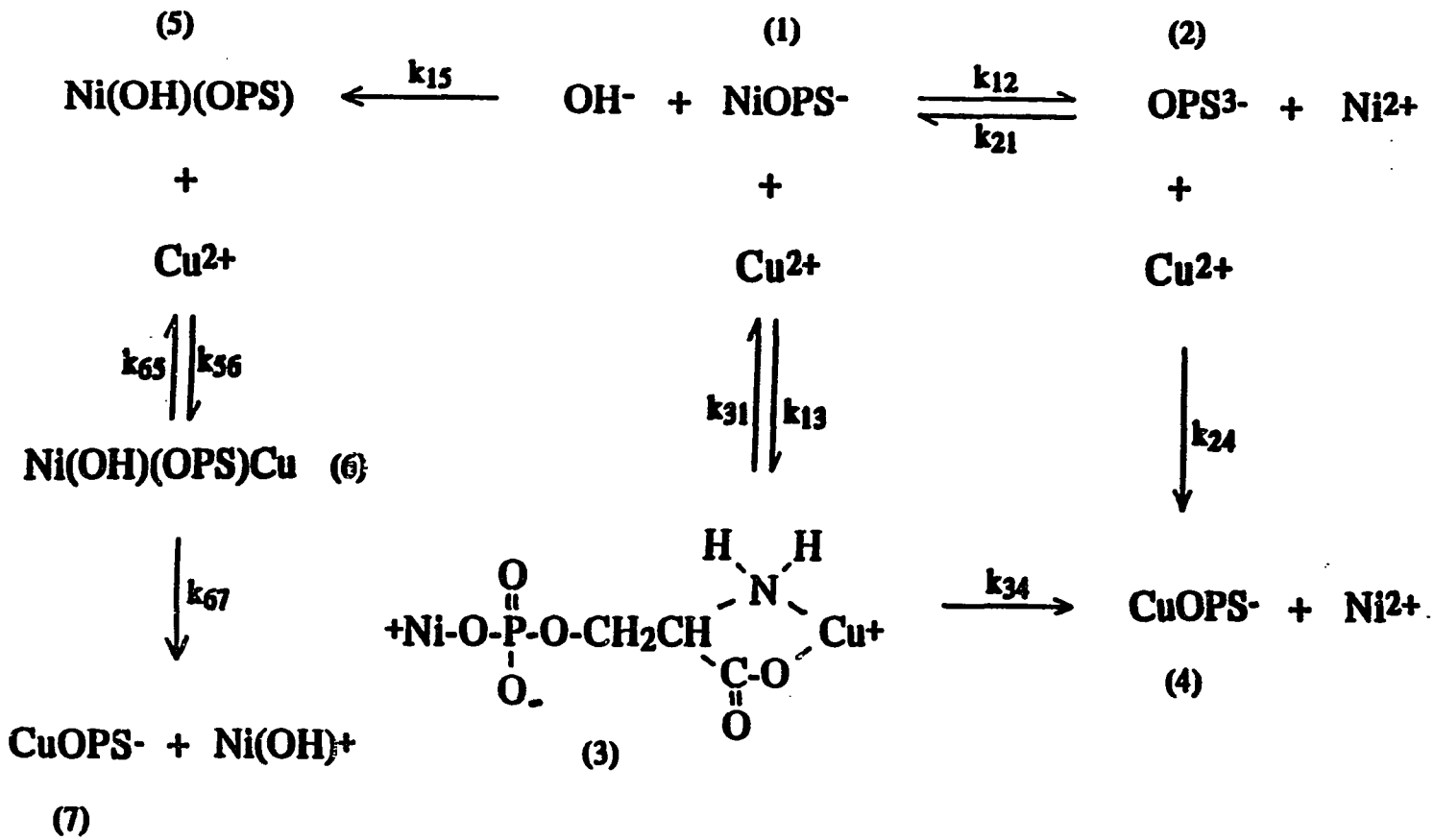

Figure 7. Proposed Mechanism for the Transfer of Ortho-phosphoserine From Nickel to Copper.

$k^{NiOPS}_{Cu^{2+}}$ and $k^{NiOPS}_{CuOH^{+}}$, depending upon the attacking species. Step 3 → 4, rupture of the nickel-oxygen bond in species 3 is the rate-determining step for the copper dependent pathway. Pathway 1 → 5 → 6 → 7 also contributes to the formation of products. Step 1 → 5, represented by $k^{NiOPS}_{OH^-}$, involves the attack of hydroxide on one of the three water molecules coordinated to $NiOPS^-$ to abstract a proton and form Ni(OH)OPS. The value of the experimental rate constant $k^{NiOPS}_{OH^-}$, 3.91×10^{10} $M^{-1}s^{-1}$, is within the range 10^{10} - 10^{11} reported by Eigen for the abstraction of a proton from a water molecule coordinated to a metal ion (32). Coordinated hydroxide has been shown to labilize subsequent reactions of nickel complexes (33). Thus, at very low hydroxide ion concentration, step 1 → 5 becomes rate limiting because pathway 5 → 6 → 7 is identical to 1 → 3 → 4 except that the former has a labilizing coordinated hydroxide attached to nickel and therefore proceeds faster. This is the reason that no copper dependency is seen in the hydroxide attack term $k^{NiOPS}_{OH^-}$.

The rate constant for the attack of $CuOH^+$ on $NiOPS^-$ shows enhanced behavior compared to that for copper as can be seen by comparing rate constants in Table 5. The

accelerating effect of hydrolyzed copper has been seen in other systems as shown in Table 9.

The explanation that has been previously set forth is that the enhanced rate of attack of $CuOH^+$ is due to the formation of some type of hydrogen-bonded or hydrogen-bridged intermediate that would impart an added degree of stability to the intermediate (11,13). In the present system, the hydroxide hydrogen could hydrogen bond to one of the oxygens in the phosphate group, or the hydroxide oxygen could form a hydrogen bond to a proton of one of the water molecules coordinated to nickel. Structure I illustrates hydrogen bonding in the dinuclear intermediate for the interaction of $CuOH^+$ with a phosphate oxygen.

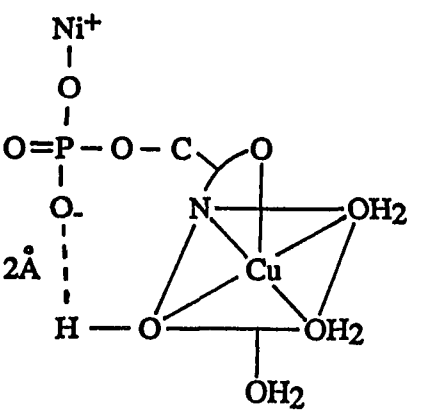

Structure I

A space-filling molecular model of Structure I was built and showed the center to center distance between the phosphate oxygen and the hydroxide hydrogen to be approximately 2Å. The strength of the hydrogen bond illustrated in Structure I or the strength of a hydrogen bond between the hydroxide oxygen and water coordinated to nickel would cause a considerable increase in the stability of the intermediate, and would be reflected in the $k^{NiOPS}_{CuOH^+} / k^{NiOPS}_{Cu^{2+}}$ ratio.

It is interesting to note that in the present system the ratio of $k^{NiOPS}_{CuOH^+}$ to $k^{NiOPS}_{Cu^{2+}}$ is 1235 and nearly identical to the ratio of 1240 for the NiEDDP system (13). In that system, a strong hydrogen bond between a free carboxylate group and the hydroxide bonded to copper was proposed to explain the large increase in rate seen in comparing $k^{NiL}_{CuOH^+}$ to $k^{NiL}_{Cu^{2+}}$.

Table 9

Comparison of Rate Constants for the Attack of Cu^{2+} and $CuOH^{+}$ on Various Complexes[a]

Complex	$k^{NiL}_{Cu^{2+}}$	$k^{NiL}_{CuOH^{+}}$	$k^{NiL}_{CuOH^{+}} / k^{NiL}_{Cu^{2+}}$
$NiBPEDA^{2+}$	4.9×10^{-4}	0.108	220[b]
$Ni(trien)^{2+}$	2.7	80	30[c]
$Ni(EDTA)^{2-}$	0.075	1.4	18[d,e]
$Zn(EDTA)^{2-}$	67	220	33[f]
$Ni(OPS)^{-}$	9.15×10^{3}	1.13×10^{7}	1235[g]
Ni(EDDP)	7.51×10^{-3}	9.29	1240[h]

[a] All rate constants in $M^{-1}s^{-1}$ at 25^{0} C.

[b] Reference 11.

[c] Reference 15.

[d] Reference 7.

[e] The data to resolve k^{NiEDTA}_{Cu} and k^{NiEDTA}_{CuOH} were not corrected for any hydrolyzed species.

[f] Reference 9.

[g] This work.

[h] Reference 13.

APPENDICES

Appendix A

Concentration and Absorbance Relationships

Concentration and Absorbance Relationships

Equation 7 relating the concentration of $NiOPS^-$ to the absorbance at any time t, A_t, the final absorbance, A_∞, and the molar absorptivities of reactants and products was derived in the following manner. The absorbance at any time, A_t, is equal to the sum of the absorbances of the reactants remaining and of the products formed.

$$A_t = \epsilon_{NiOPS^-}(b)[NiOPS^-]_t + \epsilon_{CuOPS^-}(b)[CuOPS^-]_t + \epsilon_{Ni^{2+}}(b)[Ni^{2+}]_t + \epsilon_{Cu^{2+}}(b)[Cu^{2+}]_t \quad (24)$$

The concentrations of Ni^{2+}, Cu^{2+}, and $CuOPS^-$ at any time are related to the final concentrations and the concentration of $NiOPS^-$ at any time.

$$[Ni^{2+}]_t = [Ni^{2+}]_\infty - [NiOPS^-]_t \quad (25)$$

$$[Cu^{2+}]_t = [Cu^{2+}]_\infty + [NiOPS^-]_t \quad (26)$$

$$[CuOPS^-]_t = [CuOPS^-]_\infty - [NiOPS^-]_t \quad (27)$$

Substitution of equations 25, 26, and 27 into equation 24 and rearrangement gives equation 28.

$$A_t = [NiOPS^-]_t(b)(\epsilon_{NiOPS^-} + \epsilon_{Cu^{2+}} - \epsilon_{Ni^{2+}} - \epsilon_{CuOPS^-}) + \epsilon_{Cu^{2+}}(b)[Cu^{2+}]_\infty + \epsilon_{Ni^{2+}}(b)[Ni^{2+}]_\infty + \epsilon_{CuOPS^-}(b)[CuOPS^-]_\infty \quad (28)$$

At equilibrium the absorbance due to $NiOPS^-$ is negligible, therefore, the final absorbance is expressed as follows

$$A_{\infty} = b(\epsilon_{Cu^{2+}}[Cu^{2+}]_{\infty} + \epsilon_{Ni^{2+}}[Ni^{2+}]_{\infty} + \epsilon_{CuOPS^{-}}[CuOPS^{-}]_{\infty}) \quad (29)$$

and substitution of equation 29 into equation 28 and solving for the concentration of $NiOPS^{-}$ gives the desired relation, equation 7.

$$[NiOPS^{-}]_t = \frac{A_t - A_{\infty}}{b(\epsilon_{NiOPS^{-}} + \epsilon_{Cu^{2+}} - \epsilon_{Ni^{2+}} - \epsilon_{CuOPS^{-}})} \quad (7)$$

Appendix B

Agreement Between Observed and Expected Absorbance Values to Show the Absence of Stable Intermediates

Agreement Between Observed and Expected Absorbance Values to Show the Absence of Stable Intermediates

To show the absence of any stable intermediates in the metal-exchange reaction, expected absorbance values were compared to observed absorbance values over six half-lifes as shown in Table 10. The difference between observed and expected absorbances, ΔA, can be attributed in part to cell path length (b) differences between the Cary 14, where b = 1.00 ± 0.01 cm, and the stopped-flow cell where the cell path length is 1 cm and not known with the same precision. Another contributing factor is the error in reading absorbance values from photographs, where the width of the line drawn through the traces could be significantly greater than the error in the absorbance value read from the Cary 14.

The expected absorbance values were calculated by summing the contribution to the total absorbance the absorbance of all reactants and products. Using equilibrium concentrations of all reactants and products at each half-life and the molar absorptivities given in Table 2, expected absorbances were calculated using equation 27. The

$$A_{expected} = (b)(\epsilon_{Cu^{2+}}[Cu^{2+}]_t + \epsilon_{Ni^{2+}}[Ni^{2+}]_t + \epsilon_{NiOPS^-}[NiOPS^-]_t + \epsilon_{NiHOPS}[NiHOPS]_t + \epsilon_{CuOPS^-}[CuOPS^-]_t + \epsilon_{CuHOPS}[CuHOPS]_t) \quad (30)$$

observed absorbance values were determined from %T and time data taken directly from polaroid photographs of oscilloscope traces.

Since the difference between observed and expected absorbances is nearly identical over six half-lifes, no evidence of any stable inter-

Table 10

Comparison Between Observed and Expected Absorbance Values for the Exchange Reaction of Nickel-phosphoserine and Copper(II)

Number of half-lifes	$A_{observed}$	$A_{expected}$	ΔA
1	0.0542	0.0768	0.0226
2	0.0596	0.0822	0.0226
3	0.0623	0.0848	0.0225
4	0.0637	0.0857	0.0220
5	0.0644	0.0861	0.0217
6	0.0647	0.0863	0.0216

Note. pH = 4.218, μ = 0.1 M, half-life for the exchange reaction under these conditions is 0.02 seconds.

mediates is found. The consistent difference between expected and observed absorbance values can be attributed to the fact that molar absorptivities used to calculate the expected absorbance values were determined on an instrument other than the one from which absorbances were observed.

REFERENCES

1. T.J. Bydalek and D.W. Margerum, J. Am. Chem. Soc., **1961**, 83, 4326.

2. D.W. Margerum and T.J. Bydalek, Inorg. Chem., **1962**, 1, 852-856.

3. T.J. Bydalek and D.W. Margerum, Inorg. Chem., **1963**, 2, 678-683.

4. D.W. Margerum and T.J. Bydalek, Inorg. Chem., **1963**, 2, 683-688.

5. T.J. Bydalek and M.L. Blomster, Inorg. Chem., **1964**, 3, 667-671.

6. T.J. Bydalek and A.H. Constant, Inorg. Chem., **1965**, 4, 833-836.

7. D.W. Margerum, D.L. Janes, and H.M. Rosen, J. Am. Chem. Soc., **1965**, 87, 4463-4472.

8. R.K. Steinhaus and R.L. Swann, Inorg. Chem., **1973**, 12, 1855-1860.

9. D.W. Margerum, B.A. Zabin, and D.L. Janes, Inorg. Chem., **1966**, 5, 250-255.

10. E. Mentasi and E. Pelizzetti, Inorg. Chem., **1978**, 17, 3133-3137.

11. R.K. Steinhaus and C.L. Barsuhn, Inorg. Chem., **1974**, 13, 2922-2929.

12. R.K. Steinhaus and S.H. Erickson, Inorg. Chem., **1980**, 19, 1913-1920.

13. R.K. Steinhaus, Inorg. Chem., **1982**, 21, 4084-4088.

14. J.J. Latterall, M.S. Thesis, Purdue University, **1962**.

15. P.J. Menardi, Doctoral Dissertation, Purdue University, **1966**.

16. K.W. Beyene, M.A. Thesis, Western Michigan University, **1987**.

17. G.A. Nyssen and D.W. Margerum, Inorg. Chem., **1970**, 9, 1814-1820.

18. G. Kohler and H. Elias, Inorg. Chim. Acta, **1979**, 34, L215-L218.

19. D.W. Margerum, P.J. Menardi, and D.L. Janes, Inorg. Chem., **1967**, 6, 283-289.

20. G.F. Smith and D.W. Margerum, Inorg. Chem., **1969**, 8, 135-138.

21. E.H. Abbott and M.S. Mohan, Inorg. Chem., **1978**, 17, 2203-2207.

22. H. Ohtaki and T. Kawai, Bull. Chem. Soc. Jap., **1972**, 45, 1735.

23. D.D. Perrin, J. Chem. Soc., **1960**, 3189-3196.

24. K.J. Pederson, Kgl. Dan. Vidensk. Selsk, Mat. Pys, Medd., **1939**, 20, 1.

25. L.G. Sille'n and A.E. Martell, Stability Constants of Metal Ion Complexes, Supplement No. 1, Special Publication No. 25, The Chemical Society, London, **1971**.

26. L.G. Sillen'n and A.E. Martell, Stability Constants of Metal Ion Complexes, Special Publication No. 17, The Chemical Society, **1964**.

27. H. Brintzinger and G.G. Hammes, Inorg. Chem., **1966**, 5, 1286.

28. D.B. Rorabacher, Inorg. Chem., **1966**, 5, 1891.

29. D.B. Rorabacher and A. Melendez-Cepeda, J. Am. Chem. Soc., **1971**, 3, 6071.

30. A.E. Martell and R.M. Smith, Critical Stability Constants, Plenum Press, New York, **1974**.

31. M.S. Mohan, D. Bancroft, and E.H. Abbott, Inorg. Chem., **1979**, 18, 2468-2472.

32. M. Eigen, Nobel Symposium 5, Fast Reactions and Primary Processes in Chemical Kinetics, Stig Claesson, Ed., Interscience Publishers, **1967**, p. 247.

33. S. Funahashi and M. Tanaka, Inorg. Chem., **1969**, 8, 2159-2165.